Electrical and Optical Properties of Poly(vinyl chloride)/ZnS Nanocomposites Exposed to Gamma Radiation

Nara E. Guimarães[a], Érika R. B. Ximenes[a], Lindomar Avelino da Silva[a],

Renata Francisca da Silva Santos[a], Elmo Silvano Araújo[a], Kátia Aparecida da Silva Aquino[a]*

[a]Universidade Federal de Pernambuco, Departamento de Energia Nuclear, Laboratório de Polímeros e Nanoestruturas, Recife, PE, Brasil.

Poly(vinyl chloride) (PVC) is considered one of the most versatile polymers due to its interaction with different additives. On the other hand, binary sulfides have wide applications as zinc sulfide (ZnS), one of the first discovered semiconductors. This study aims to synthesize a nanocomposite material containing nano ZnS in the PVC matrix with a surfactant as a compatibilizer agent to evaluate its optical and electrical properties when exposed to gamma radiation. Our results showed that adding ZnS at 0.5 wt% concentration in the PVC matrix promoted the system from insulating to the semiconductor material. Therefore, gamma radiation has played an important role in nanocomposites' optical and electrical properties with changes in electrical and electrical conductivity, constant dielectric parts, refraction index, optical band gap, and Urbach energy. Thus, our study points to the development of nanocomposite material, semiconductors, and features useful for applications in flexible electronics or optical-electronic devices.

Keywords: *Optical-electronic devices, gamma radiation, gap band.*

1. Introduction

Electronics have been undergoing a disruptive evolution, investing in lightweight, soft and flexible devices instead of heavy, bulky, and rigid devices[1]. Thus, flexible electronics is a fast-growing field that promises to develop new commercial products such as displays, solar cells, and biomedical sensors. These devices can be incorporated into clothing and other everyday items that ensure they revolutionize our daily lives[2]. In this way, the electronic industry opens up new opportunities, and endless manufacturing advances in thin-film materials and devices will make flexible electronics ubiquitous[3].

Usually, flexible electronic devices take advantage of the mechanical properties of conventional plastics and the semiconductor properties of conjugated polymers[4-6]. Many polymers exhibit high flexibility, low density, and transparency. Some are biocompatible and biodegradable and therefore are the dominant materials in flexible electronics.

Most polymer materials are electrical insulators in nature. Moreover, polymer nanocomposites offer a new possibility for improving electrical conductivity. These materials can become conductors through different methods: i) the creation of conjugated double bonds in the polymer main chain; ii) the introduction of the donor-receptor complex in the polymer matrix; iii) the addition of conductive charges such as metallic powders and carbon black[3]. Employing inorganic nanoparticles combined with commercially available polymer extends the range of conductive materials.

One of the goals of materials research is to create new materials with physical properties tailored to a specific application and to understand the mechanisms that control these properties. Irradiation techniques are an advanced method for modifying materials. It is well known that electrical conduction in polymers can be considerably increased by irradiation[7-12]. Polymer nanocomposites with adjustable electrical and optical properties by gamma radiation have many applications in flexible electronics. For example, El-Shamy et al.[8] studied the influence of gamma radiation on the electrical and dielectric properties of poly(vinyl acetate)/silver nanocomposite films. The results showed that the value of the dielectric constant of the films decreased with the increase in gamma radiation doses. Thus, gamma radiation doses increase the material's electrical conductivity and alter its conduction behavior. In this way, inorganic loadings were already used as additives for polymers exposed to gamma radiation to improve chemical, thermal, and mechanical properties[13,14].

The polymer nanocomposites have gained importance in manufacturing products with high-performance properties for different industries. An important polymer is poly(vinyl chloride) (PVC), which is a synthetic polymer with applications in diverse fields such as blood tubes, blood bags, consumer goods, cable insulation, etc[15]. Moreover, the semiconductors nanoparticles offer a new possibility for improving optical and electrical properties when incorporated into the PVC matrix[16,17]. However, PVC molecule changes upon gamma radiation with dose-dependence in crosslinking and scission

*e-mail: aquino@ufpe.br

effects in the main chain. The development of crosslinking results in the joining of adjacent PVC chains to form a three-dimensional network in which radicals recombine with each other. Oppositely, chain scission occurs whenever the radicals fail to recombine resulting in a reduced molecular chain[13,18].

On the other hand, zinc sulfide (ZnS) is the first semiconductor discovered and has been gaining extensive attention for its luminescence properties, low absorption coefficient in the visible and near-infrared region, good dielectric properties, and high refractive index. For this reason, ZnS has a variety of applications, including light-emitting diodes, electroluminescence, flat-panel monitors, sensors, lasers, bio-devices, and infrared windows, featuring good chemical stability and physical resistance with rapid electronic response[19,20].

In this way, this study aims to investigate the effects of gamma radiation on the optical and electrical properties of a nanocomposite containing ZnS nanoparticles (dispersed with octadecylamine) in the PVC matrix. It was expected to produce a new material once gamma radiation improved optical and electrical properties have become increasingly important in the electronics industry.

2. Materials and Methods

2.1. Experimental part

The poly(vinyl chloride) (PVC) produced by Braskem (Brazil) was utilized in this study. According to Braskem, the PVC in this study is a resin without processing additives and polymerized by the suspension method. A known amount (1.8g) of PVC; was dissolved in 40 ml of the methyl-ethyl-ketone (MEK) as the solvent and stirred by a magnetic stirrer for 24h at 60⁰C to form a homogenous solution. This step was repeated by adding a required quantity of ZnS nanopowder as a loading to the PVC solution to create films at 0.3; 0.5; 0.7; and 1.0 wt% concentrations. Moreover, octadecylamine was added to solutions in a similar amount of ZnS quantity to improve nanoparticle dispersion in the polymer matrix. The ZnS was synthesized and characterized in our previous study, showing a spherical shape with diameters ranging from 2 to 3 nm[21]. After the magnetic stirrer, the films were obtained by the casting method. The Petri dishes were stored in a cabinet with a dehumidifier at room temperature (≈ 27 ⁰C). The PVC and PVC/ZnS nanocomposites films were peeled from Petri dishes and kept in desiccators until use.

Digimess digital micrometer with an accuracy of 0.004 mm was carried out to determine the thickness of the films. PVC and PVC/ZnS nanocomposites films were irradiated with gamma radiation. The gamma rays were from a non-attenuated 60-Co source (Gammacell GC220 irradiator - MDS Nordion, Canada), at 25, 50, and 75 kGy doses in air, the dose rate of 2.66 kGy/h, and at room temperature (≈ 27ºC).

The electrical resistance (R') of PVC and PVC/ZnS films (1.5 x 0.5 cm, and quadruplicated samples), irradiated and unirradiated, was measured by two probe techniques using a digital Keithley electrometer, 6517 A, 200Ω resistance standard, with the direct current source. The silver paste was used to ensure good contact of the sample surface with electrodes. Two metal claws were placed on the electrodes that connect the films to the electrometer. The R' value (Ω)

was obtained direly from the equipment. The specific volume resistivity (ρ_v) of films was obtained using Equation 1[22].

$$\rho_V = \frac{2.27 \times R' \times t^2}{d \times \cosh^{-1}\left(\frac{d}{d_0}\right)} \quad [\Omega.m] \tag{1}$$

Where t is film thickness (mm), d_0 is electrode diameter (in this study, d_0=1.48 mm), and d is the distance between electrodes. In this study d=12.15 – 2 (d_0/2), i.e., d=10.67 mm.

Finally, the films' specific electrical conductivity (σ) values were estimated using Equation 2[23]. In this study, the following ranges of electrical conductivity were adopted: $\sigma \leq 10^{-6}$ S. m^{-1} (insulating), $10^{-5} < \sigma < 10^2$ S.m^{-1} (semiconductor), and $\sigma > 10^2$ S. m^{-1} (conductor)[24].

$$\sigma = \frac{1}{\rho_v} \quad [S.m^{-1}] \tag{2}$$

In addition, the optical absorption spectrum is one of the essential tools for understanding the electronic and optical properties of pure and doped polymers. The spectra were carried out with JASCO V-730 UV-visible/NIR spectrophotometer in the wavelength range 230–800 nm with an accuracy of ±0.2 nm at 18⁰C. Thus, the optical properties of films (irradiated and unirradiated) were estimated from UV-visible spectra according to equations shown in the optical absorption theoretical part below.

2.2. Optical absorption theoretical part

Measuring the absorption of UV-vis spectrum is the most direct method for investigating some optical properties of materials. In the photon absorption process, electrons in a molecule are excited from one energy level to a higher energy level, featuring the following molecular electronic transitions types: $\sigma \rightarrow \sigma*$, n $\rightarrow \sigma*$, n $\rightarrow \pi*$, and $\pi \rightarrow \pi*$. These transitions were referred to as band-to-band or exciting transitions. Furthermore, the absorption edge is the fundamental absorption manifested by electron excitation from the valence band to the conduction band, evaluated from the maximum peak position in UV-vis spectra[25].

The absorptions (A) obtained from UV–vis spectra can be used to determine the optical band gap (E_g) since the absorption coefficient (α) depends on the frequency of absorbed photon (ν) and can be defined by Beer–Lambert's law[25,26]:

$$\alpha = 2.303 \frac{A}{t} \quad [cm^{-1}] \tag{3}$$

Where t is the thickness of the film in centimeters (cm). On the other hand, the absorption coefficient (α) is related to photon energy ($h\nu$) and optical band gap (E_g) by Tauc's relation[26-29]:

$$(\alpha h\nu)^{\frac{1}{m}} = B\left(h\nu - E_g\right) \tag{4}$$

Where $h\nu$ is the incident photon energy (approximately $h\nu = 1240/\lambda$), B is a constant, and m corresponds to the band gap transition type that depends on the nature of the

material[25,30]. The m value exhibits 1/2 for allowed direct transition, 2 for indirect allowed transition, 3/2 for direct forbidden transition, and 3 for indirect forbidden transition[30]. The absorption coefficient's dependence on the photon energy helps study the type of electrons transition[31]. Thus, when the values of the absorption coefficient of material are high ($\alpha \geq 10^4$ cm^{-1}) it is expected that direct (allowed and forbidden) transitions of the electron to happen. Oppositely, i.e., when $\alpha < 10^4$ cm^{-1}, the indirect (allowed and forbidden) transitions of the electron are expected[32,33].

On the other hand, the carbonaceous cluster is one of the important parameters analyzed to enhance the optical properties of the polymeric material. This cluster is rich with a charge carrier, which enhances the surface conductivity of the polymers. The size of the cluster in irradiated polymers is more extensive, and the number of carbon atoms in hexagon rings per conjugation length (M) can be found using Equation 5[34].

$$M = \left(\frac{34.3(eV)}{E_g(eV)}\right)^2 \tag{5}$$

The numeric value (34.3 eV) is associated with π–π* optical transitions in band structure energy (-2.9 eV) of a pair of adjacent π bond sites in –C=C– ligation for hexagon rings in buckminsterfullerene form.

Near the band edge in UV-vis spectra, the α depends exponentially on the photon energy and obeys the empirical Urbach rule[35]. This rule can be used for determining Urbach's energy (E_U). The E_U is the width of the band tails of localized states in the customarily forbidden band gap, associated with the structural defects and disorder within the polymer matrix. The origin of the E_U is considered as thermal vibrations in the lattice[36]. The E_U can be determined using Equation 6[35].

$$\alpha = \alpha_o \exp\left(\frac{h\nu}{E_U}\right) \tag{6}$$

Where α_o is a constant that characterizes the materials, the E_U could be estimated from the reciprocal of the straight-line slope of lnα versus $h\nu$ plot.

The Reflectance (R) of the surface of the films is a component of the response of the material's electronic structure to the electromagnetic field of light and depends on the wavelength of light. Using the absorption value (A) is possible to obtain transmittance (T=10^{-A}) of the material, and then the R of the films was determined by Equation 7[37].

$$R = 1 - \sqrt{T \cdot e^A} \tag{7}$$

Where e = Euler's number.

The refractive index (n) of a material is one of an optical material's most significant defining properties. It measures how the speed of light changes as it travels from a vacuum into a material. The n in non-magnetic material is dependent on the dielectric constant and other factors such as temperature as the introduction of loadings in the system, for example. The R data was used to calculate the n by Equation 8[38].

$$n = \frac{1+\sqrt{R}}{1-\sqrt{R}} \tag{8}$$

The extinction coefficient (k) is related to a fraction of energy lost due to absorption and scattering per unit thickness. The k was evaluated using equation eight from wavelength (λ) of absorbance data[39].

$$k = \frac{\alpha \lambda}{4\pi} \tag{9}$$

The variation in n and k values as a function of wavelength reveals that some interaction occurs between electrons of the film molecules and incident photons. These parameters have an intrinsic relationship with the dielectric constant of the material.

The dielectric constant is a dimensionless parameter that describes its tendency to polarize in response to an applied electrical field. The complex dielectric constant ($\varepsilon* = \varepsilon r + i\varepsilon i$) is a fundamental property. Thus, the dielectric constant characterizes the optical properties of solid material and consists of two components: the real part (εr) and the imaginary part (εi). The real part of the dielectric constant is related to the speed of light in the material that is interrelated to its electronic polarization, whereas the imaginary part indicates dipole motion due to absorption energy from an electric field. The k and n values were used for the obtention of the real and imaginary parts of the dielectric constant by Equations 10 and 11, respectively[39]:

$$\in r = n^2 - k^2 \tag{10}$$

$$\in i = 2nk \tag{11}$$

Finally, the optical conductivity (σ_{opt}) is related to the movement of the charge carriers by the alternating electric field of the incident electromagnetic waves, which is given by Equation 12[40].

$$\sigma_{opt} = \frac{\alpha n c}{4\pi} \tag{12}$$

Where c = 3x10^{10} cm/s (velocity of light).

3. Results and Discussion

3.1. Electrical conductivity

Table 1 despite the influence of ZnS and gamma radiation on the electrical conductivity of PVC films. The PVC and PVC/ZnS films produced had a thickness of around 0.128 ± 0.03 mm with a slight increase for ZnS concentration at 0.7 and 1.0 wt%. Each point represents the average of the four measurements (different films). As expected, unirradiated PVC films showed insulating behavior with an electrical conductivity value of 2.9 x 10^{-9} ± 1.2 x10^{-9} S/m without significant changes before gamma radiation. Nevertheless, the electrical conductivity of unirradiated PVC/ZnS systems is increased on ZnS content, probably by the formation of charge-transfer complexes in the film. In this way, only the films at 0.5 wt% concentration became a semiconductor system with an electrical conductivity value of around 1.6 x 10^{-5} ± 4.5x10^{-6} S/m. The interface adhesion and/or bonding between the polymer matrix and the dispersion

Table 1. Influence of Irradiation dose and ZnS concentration on the electrical conductivity of PVC and PVC/ZnS films.

Zn Concentration (wt%)	Thickness (mm)	Electrical conductivity (S/m)			
		0 (kGy)	25 (kGy)	50 (kGy)	75 (kGy)
0	0,127	2.9×10^{-9}	1.1×10^{-9}	1.3×10^{-9}	8.8×10^{-9}
	±0,034	$\pm1.2\times10^{-9}$	$\pm2.0\times10^{-10}$	$\pm3.0\times10^{-10}$	$\pm3.0\times10^{-10}$
0.1	0,127	7.7×10^{-7}	1.3×10^{-5}	1.9×10^{-9}	7.5×10^{-9}
	±0,016	$\pm9.2\times10^{-8}$	$\pm5.0\times10^{-6}$	$\pm1.4\times10^{-10}$	$\pm4.0\times10^{-10}$
0.3	0,128	1.1×10^{-6}	6.6×10^{-5}	2.5×10^{-5}	3.8×10^{-9}
	±0,004	$\pm6.3\times10^{-7}$	$\pm4.0\times10^{-6}$	$\pm2.4\times10^{-6}$	$\pm1.2\times10^{-10}$
0.5	0,125	1.6×10^{-5}	3.7×10^{-5}	2.3×10^{-5}	1.0×10^{-9}
	±0,024	$\pm4.5\times10^{-6}$	$\pm1.3\times10^{-6}$	$\pm3.3\times10^{-6}$	$\pm3.1\times10^{-10}$
0.7	0,131	1.1×10^{-8}	4.0×10^{-5}	1.5×10^{-5}	1.7×10^{-8}
	±0,006	$\pm3.6\times10^{-9}$	$\pm3.5\times10^{-6}$	$\pm2.3\times10^{-6}$	$\pm2.0\times10^{-9}$
1	0,131	8.8×10^{-7}	3.3×10^{-5}	1.1×10^{-5}	1.1×10^{-8}
	±0,034	$\pm1.2\times10^{-8}$	$\pm2.1\times10^{-6}$	$\pm4.1\times10^{-6}$	$\pm1.5\times10^{-9}$

of ZnS nanoparticles seem more significant at 0.5 wt% concentration. Thus, the movement of ZnS along PVC chains produces conductivity.

On the other hand, at a higher concentration than 0.5 wt%, the electrical conductivity values are somewhat decreased. This behavior may be ascribed to some ZnS agglomerates that partially contributed to reducing the mobility of the electric charges[41]. Our previous study identified the small ZnS agglomerations in SEM micrographs of PVC/ZnS[21].

Also, according to Table 1, gamma radiation plays an important role in the electrical conductivity of all nanocomposite films, particularly at 25 and 50 kGy doses. Our early study found that the PVC films undergo predominantly main chain scission at 25 and 50 kGy this effect facilitates the movement of nanoparticles along the polymer matrix increasing the electrical conductivity of the films. Further, ZnS nanoparticles act as energy-absorbing centers during exposure to gamma rays[21]. This absorption manifests in any localized redistribution of ZnS in the host polymer chain with the presence of more contacts between individual nanoparticles. All films irradiated at 25 and 50 kGy doses went from insulators to semiconductors (highlighted in Table 1).

Furthermore, a significant effect of gamma radiation was found at 25 kGy with a substantial increase in electrical conductivity for low ZnS concentration (0.1 wt%). The chances of interactions between the polymer and gamma rays are more likely in samples with a low load concentration. For this reason, it was found that the value of electrical conductivity increased for ZnS concentrations to lower than higher. However, the damage to the PVC matrix was more pronounced at a 50 kGy dose. Thus, several events in the polymer matrix could influence the decrease of nanocomposites' electrical conductivity compared with films irradiated at 25 kGy.

It is well known that the behavior of PVC is dependent on dose radiation[42]. Thus, it was expected that the crosslinking effect was predominant at the 75 kGy dose, and the electrical conductivity value of nanocomposites was significantly decreased. The possible explanation is that the crosslinking effect leads to reduced PVC chain mobility and, consequently, reduced mobility of the ZnS nanoparticles. In turn, the electrical conductivity is sensitive to the motion of charged species such as ZnS.

3.2. Optical properties

3.2.1. Absorption study

The optical properties of PVC and PVC/ZnS films, irradiated and unirradiated, were recorded by UV-vis spectroscopy (Figure 1). Analysis of the absorption spectrum in the lower energy region gives information about atomic vibrations, while the higher energy region of the spectrum provides knowledge about electronic states in the atoms[38].

The absorbance of films increases with both ZnS concentration and irradiation dose. The increased absorbance in unirradiated films is caused by the ZnS nanoparticles that acted as scattering centers in the PVC matrix. On the other hand, the absorbance increases significantly for irradiated films due to changes in the molecular structure of the PVC matrix induced by gamma radiation[43,44]. These changes were formed when PVC molecules break in chlorine bonds, removing hydrochloric acid and forming double bonds in the chain[13,21,42]. Other damages were generated, leading to new defects and new charge states. Consequently, the defects and double bonds are also referred to as color centers (chromophore group) and impact films' light absorption[45].

These effects can lead to more significant interchain interactions increasing the localized state density. These changes were more pronounced for ZnS concentration at 0.7 and 1.0 wt% due to broadening the edge peak. Thus, lower energy was required for the optical transition, and the absorption moved towards longer wavelengths[46].

In addition, the regular change in the absorbance of the PVC/ZnS films provides evidence for the good dispersion of nanoparticles (or some aggregates) in the PVC matrix[47], reinforcing the action of octadecylamine as a nanoparticle dispersant. This result follows SEM micrographs of PVC/ZnS discussed in our previous study[21].

The UV-vis absorption of unirradiated PVC films showed an absorption edge at 279 nm assigned to the n–π* transition of -Cl group in PVC molecule[33]. The absorption edge for all curves is shifted towards longer wavelengths with increasing ZnS content. This phenomenon may be attributed to the complexation between the dopants and the PVC[21,33] and the change in polymer molecular structure by gamma radiation effects.
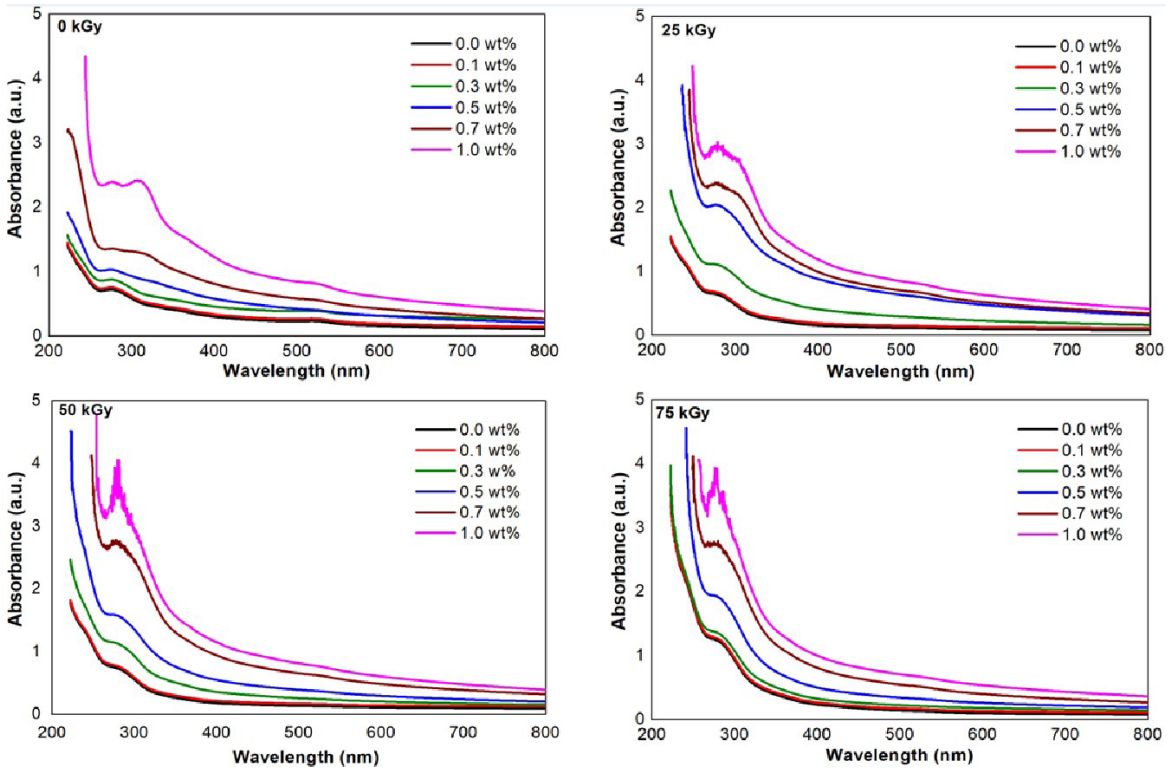
Figure 1. UV-vis spectra of PVC and PVC/ZnS nanocomposites films.

The absorption edge is the region when an electron jumps from a state with low energy to a state with higher energy due to photon absorption[41]. The materials enable light absorption in the absorption edge region, and the quantity is measured from the optical absorption coefficient (α). The physical meaning of α is the fractional attenuation of photon energy per unit distance. Figure 2 shows the relation between α and photon energy for the sample. It was found that the absorption edge value shifts from 4.18 eV for PVC to lower values for PVC/ZnS films for unirradiated films. The decrease in edge energy does mean that lower energy is required to transfer the electrons from the valence band (VB) to the conduction band (CB) of nanocomposite films. The enhancement of carrier–carrier interaction due to the ZnS presence in PVC matrix results in the absorption edge shifting. Similar results were found for whole irradiated films.

3.2.2. Transmittance analysis

Figure 3 shows the effects of the ZnS concentration and radiation dose in the optical transmittance of PVC films. To elucidate the dependence of optical behavior of PVC and PVC/ZnS films, we analyze the transmittance in two distinct spectral regions: the high-energy region ($\lambda \leq$ 350 nm) and the low-energy ($\lambda >$ 350 nm). The Figure shows that the transmittance intensity of PVC and PVC/ZnS films (irradiated and unirradiated) is relatively low in the high-energy region, but the films exhibit high transmittance in the low-energy region.

Analyzing Figure 3 in the two regions of unirradiated systems, a decreased optical transmittance was observed as increased ZnS content in the PVC/ZnS films. The reduced transmittance could be caused by increasing localized state density in the high-energy region. On the other hand, in the low-energy region, the optical transmittance reduction could be attributed to nanoparticle agglomerations caused by increasing ZnS content in the PVC matrix[21]. This nanoparticle behavior leads to optical transitions resulting in energies absorbed in the visible part of spectra[45,46].

Furthermore, when PVC and PVC/ZnS films were exposed to gamma-rays in the high-energy region, the optical transmittance of films decreased with an increase in irradiation dose. The reduced transmittance could be attributed to the rise of disorder caused by scission or crosslinking effects in this region. Similar results were found for PVC/ZnS films at 0.5, 0.7, and 1.0 wt% concentrations in the low-energy region. However, in the visible region, it enhanced the transparency for both PVC and PVC/ZnS films at 0.1 and 0.3 wt%. Probably, this effect was influenced by defects caused by gamma radiation to the polymer matrix and the more mobility of ZnS in the lower concentrations.

3.2.3. Refractive index analysis

The refractive index is an optical material's most significant defining property. In this study, the refractive index (n) in the visible region (λ=500 nm) for unirradiated PVC film is 1.46, which is consistent with values measured in other studies[47,48]. However, Table 2 reveals the refractive index as a function of ZnS concentration and irradiation dose. For PVC/ZnS films unirradiated, the n increased with increasing ZnS concentration. Similar behavior was found
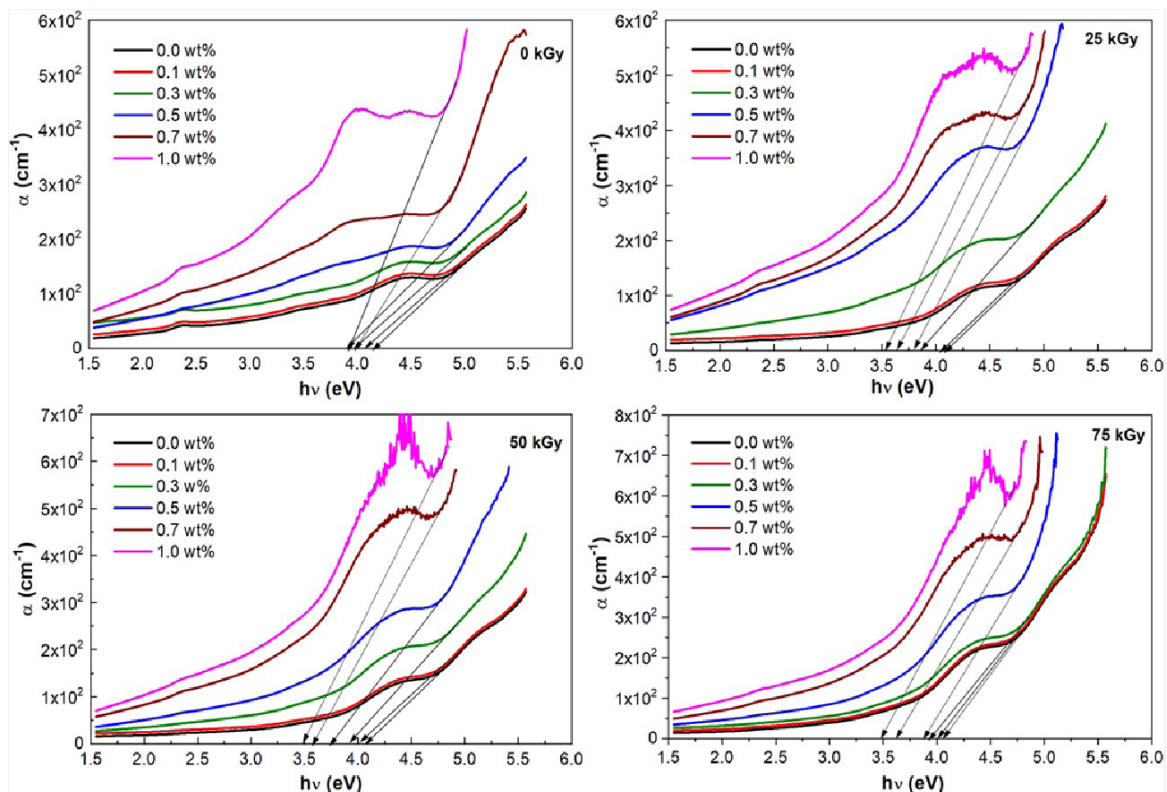
Figure 2. Absorption coefficient of PVC and PVC/ZnS nanocomposites films.
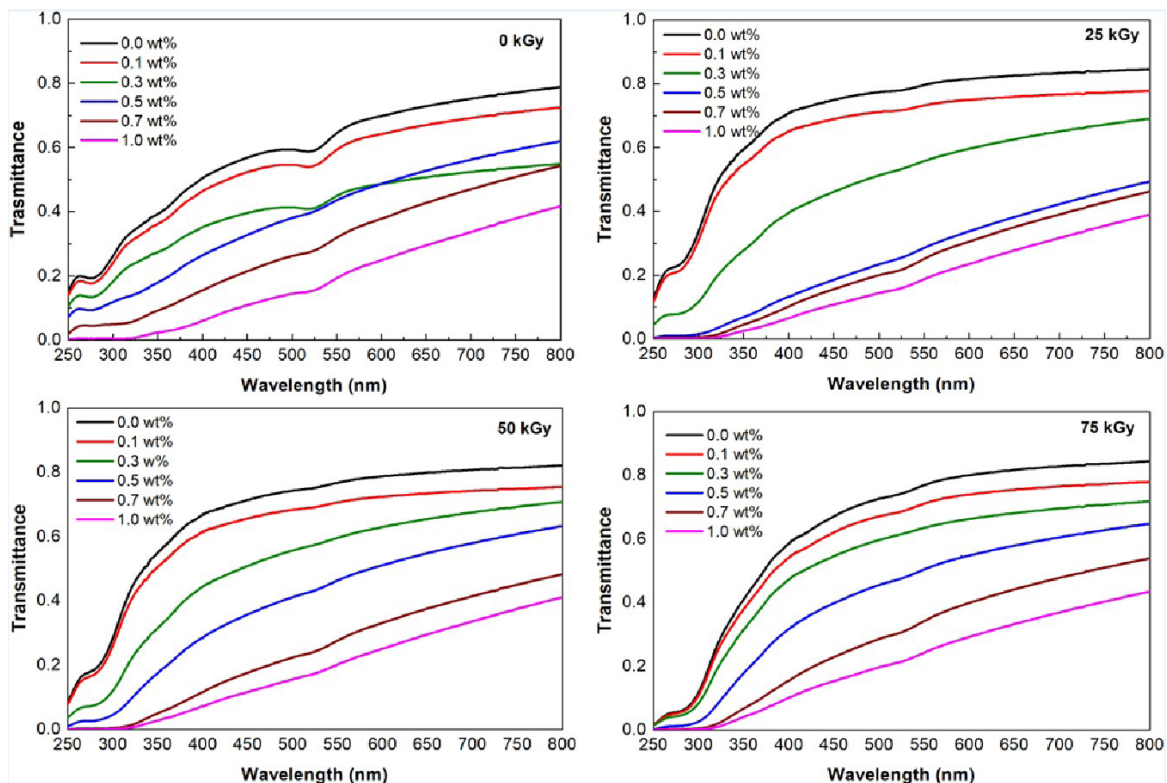
Figure 3. Influence of ZnS concentration and gamma radiation on the optical transmittance of PVC films.

Table 2. Relationship between refractive index (n) and extinction coefficient (k) with ZnS concentration for unirradiated and irradiated films at λ=500nm.

Dose	0.0 wt%		0.1 wt%		0.3 wt%		0.5 wt%		0.7 wt%		1.0 wt%	
	n	K x 10^{-5}	n	K x 10^{-5}	n	K x 10^{-5}	n	K x 10^{-5}	n	K x 10^{-5}	n	K x 10^{-5}
0	1.46	1.6	1.48	1.9	1.53	2.7	1.55	2.9	1.62	4.1	1.71	6.0
25	1.40	0.8	1.42	1.0	1.49	2,1	1.64	4.5	1.67	4.9	1.71	6.0
50	1.41	0.9	1.43	1.2	1.47	1.8	1.54	2.7	1.65	4.6	1.70	5.8
75	1.41	0.9	1.43	1.2	1.46	1.6	1.51	2.4	1.61	3.9	1.67	5.0
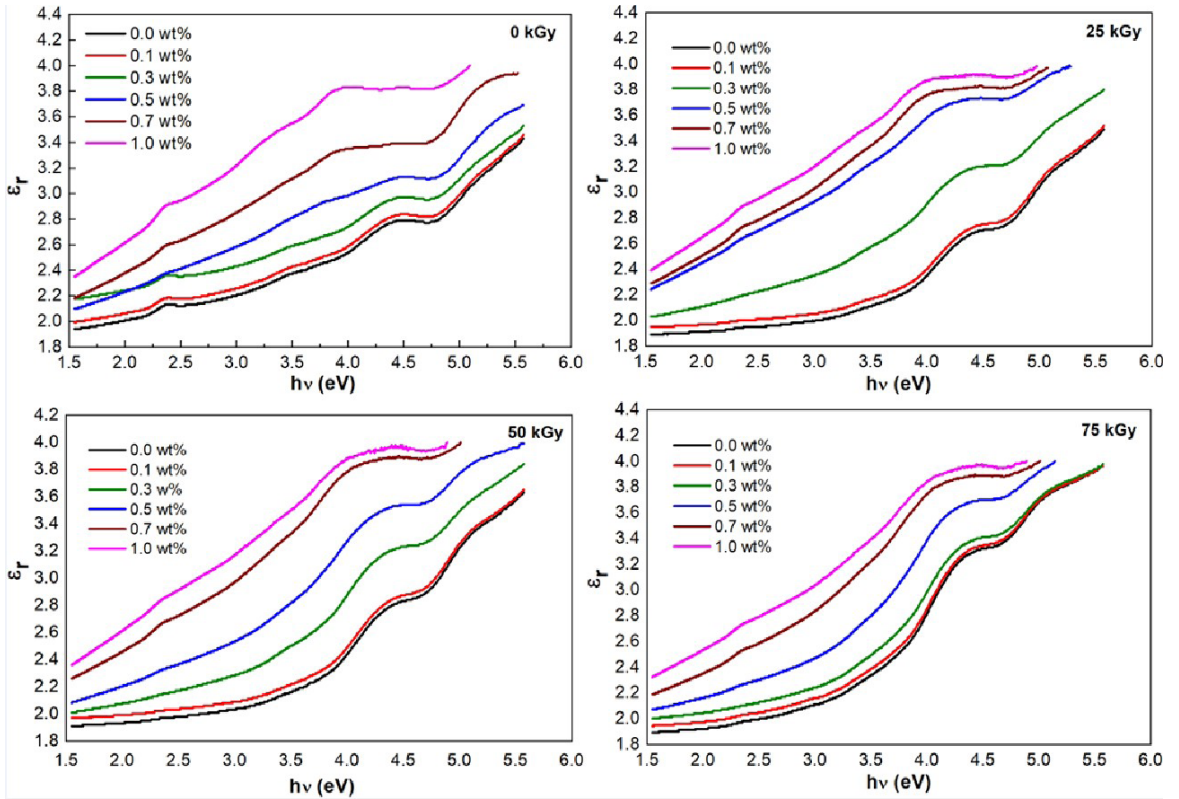
Figure 4. Influence of gamma radiation on optical dielectric real part (ε_r) of PVC and PVC/ZnS films.

for irradiated nanocomposites films. The increase in the n value of PVC/ZnS films means phase velocity deceleration due to the incorporation of the nanoparticles into the films resulting in a density increment[31].

However, the n value of PVC and PVC/ZnS films decreased with the increase of radiation dose, i.e., the changes in PVC molecular weight distribution by irradiation play an important role in n values. The main chain scission and crosslinking effects could vary the orientation of chains, thus altering films' refractive index. The crosslinking effect, for example, provoke tightness and closeness between chains. The formation of intermolecular crosslinking, for example, increased the density of the film, i.e., decreased the anisotropic character of the nanocomposite films[49].

The n value changes showed that the ZnS incorporation in the PVC matrix is the acceptable approach to tailor the refractive index efficiently. It has potential applicability for optical devices in optical waveguides, camera lenses, photonic devices, optical reflectors, etc[50,51]. In addition, the increase in the k value in the ZnS concentration function indicates more photons scattering on the film's surface. However, the k values decreased as a dose function probably by new ZnS dispersion in the polymer matrix due to radiation effects in the PVC molecule.

3.2.4. Optical dielectric constant and optical conductivity study

The optical dielectric constant has a dependence on n and k values. The dielectric constant for PVC film increased due to the ZnS concentration and irradiation dose of the real part (Figure 4) and the imaginary part (Figure 5). Furthermore, the dielectric constant values increased with increasing photon energy. These behaviors indicating interfacial polarization were increased due to the heterogeneous structure of nanocomposites due to PVC interaction with ZnS[52].
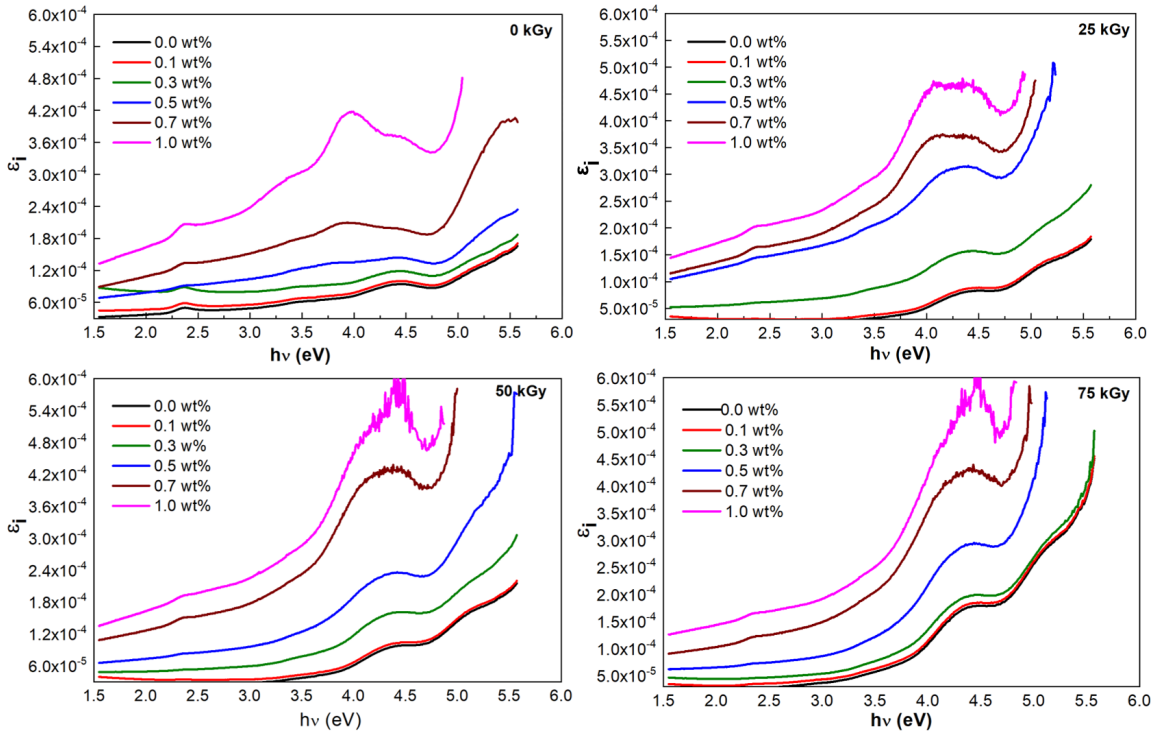
Figure 5. Influence of gamma radiation on optical dielectric imaginary part (ε_i) of PVC and PVC/ZnS films.

In addition, the dielectric behavior of irradiated films is explained by the presence of an appreciable number of defects in the PVC matrix due to the chain scission or/and crosslinking effects[42]. This means that increased defect forms a more significant number of dipoles that govern the dielectric properties of irradiated PVC and PVC/ZnS films[53].

On the other hand, the optical conductivity (σ_{opt}) informs the movement of the charge carriers by an alternating electric field of the incident electromagnetic waves. The influence of ZnS concentration and irradiation dose on the σ_{opt} of films is shown in Figure 6. The σ_{opt} increases with an increase of both ZnS concentration and irradiation dose. These results could be due to new levels within the band gap. This effect facilitates shifts of the electrons from the valence band to the conduction band[54] due to photon-atom interaction. Moreover, the σ_{opt} values decrease with the increase of wavelength.

3.2.5. Band gap and Urbach's energies study

The photon and electron interaction in the system is interpreted based on perturbation in the ground electronic state. Thus, the photon emission and absorption cause transitions between the filled and unfilled levels[31]. The band gap (E_g) is an energy range without electronic levels lying between the conduction band (CB) and valence band (VB). To create transitions between these two bans of energy, it required adequate energy, i. e., the energy that permits the transport of the mobile carrier species between the VB and CB by electrons.

This study used a combination of techniques to determine the E_g values, i. e., Tauc's model, and optical dielectric imaginary parameter (ε_i) analysis. Tauc's model is a well-known method to measure E_g values, and identify the electron transition types with the aid of the ε_i parameter study[31,55-58]. The ε_i parameter is related to the transitions between valence and conduction bands once it is correlated to an electronic absorption of the materials[59-61].

It is documented that edge absorption energy obtained from ε_i spectra is used to provide the E_g[62]. Thus, the optical ε_i plots versus the energy of the photons for whole films shown in Figure 5 were analyzed. The E_g was obtained from extrapolating the linear part of ε_i to zero. On the other hand, the adsorption coefficient (α) analysis in response to the photon wavelength depended on Tauc's relation[32,33]. As shown in Figure 2, the absorption coefficient of PVC film is less than 10^4 cm^{-1} indicating that indirect transitions may be predominant in all systems. However, the usual method for determining the value of E_g for PVC and its nanocomposites involves direct transition analysis[27-30]. In this way, the plots of $(\alpha h\nu)^{1/m}$ versus $h\nu$ only for m=1/2 (direct allowed transition) and m=2 (indirect allowed transition) were analyzed. The plots enable us to estimate E_g by extrapolating the linear part of $(\alpha h\nu)^{1/m}$ to zero. The Eg values for direct allowed transitions and indirect allowed transitions have been analyzed from the plots in Figures 7 and 8, respectively.

Table 3 shows the measured E_g values for PVC and PVC/ZnS films (irradiated and unirradiated) obtained by Tauc's model and ε_i plot. The values obtained by ε_i and $(\alpha h\nu)^{1/2}$ plots are relatively less than to E_g values attained from the $(\alpha h\nu)^2$ plot, probably because indirect allowed transitions were happening more easily in the systems. In addition, the E_g value found by the ε_i plot is very close to the absorption edge value found in Figure 2 .
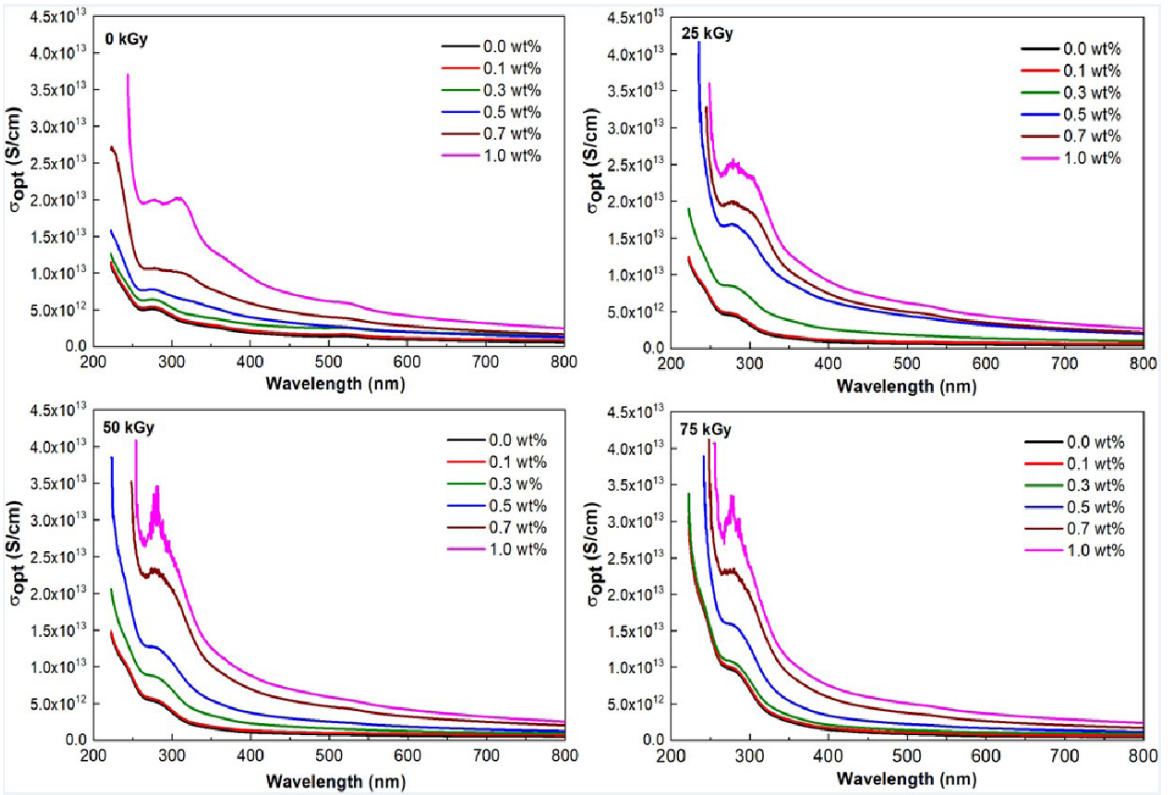
Figure 6. Influence of gamma radiation on the optical conductivity (σ_{opt}) of PVC and PVC/ZnS films.
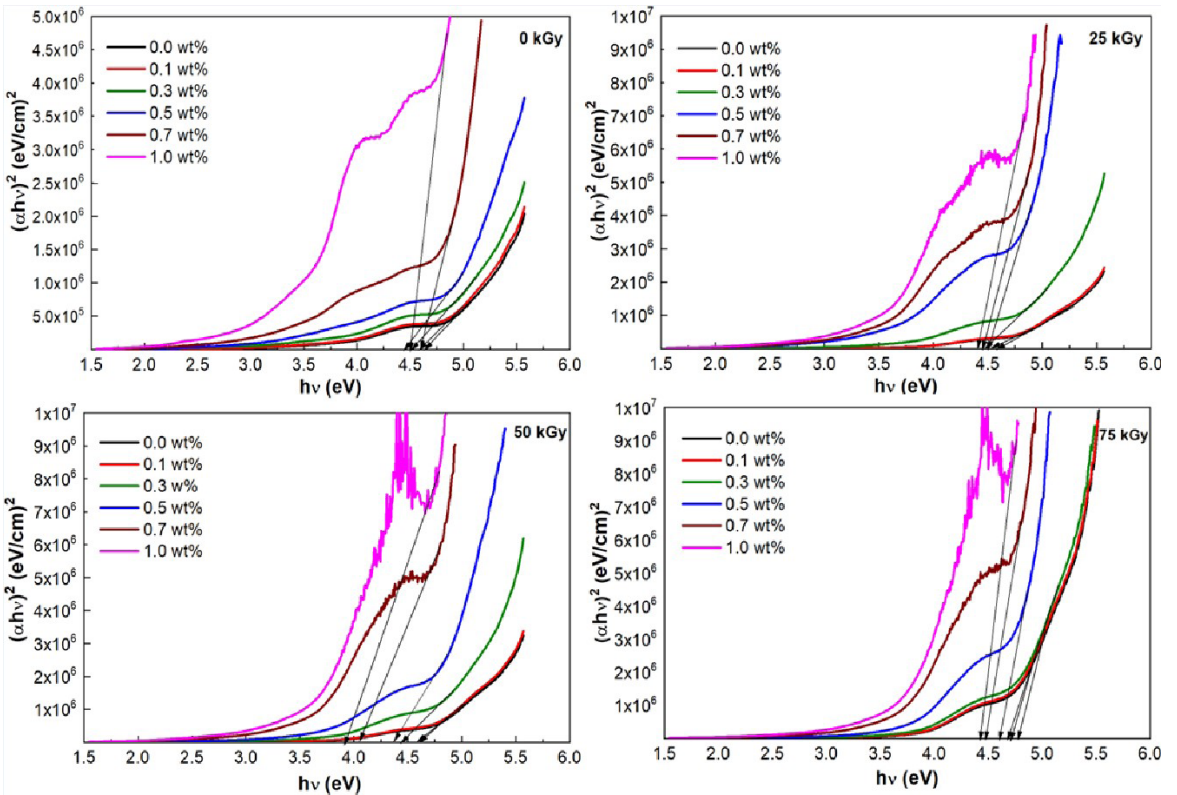
Figure 7. Plot of $(\alpha h\nu)^2$ versus $h\nu$ for irradiated and unirradiated PVC and PVC/ZnS films.
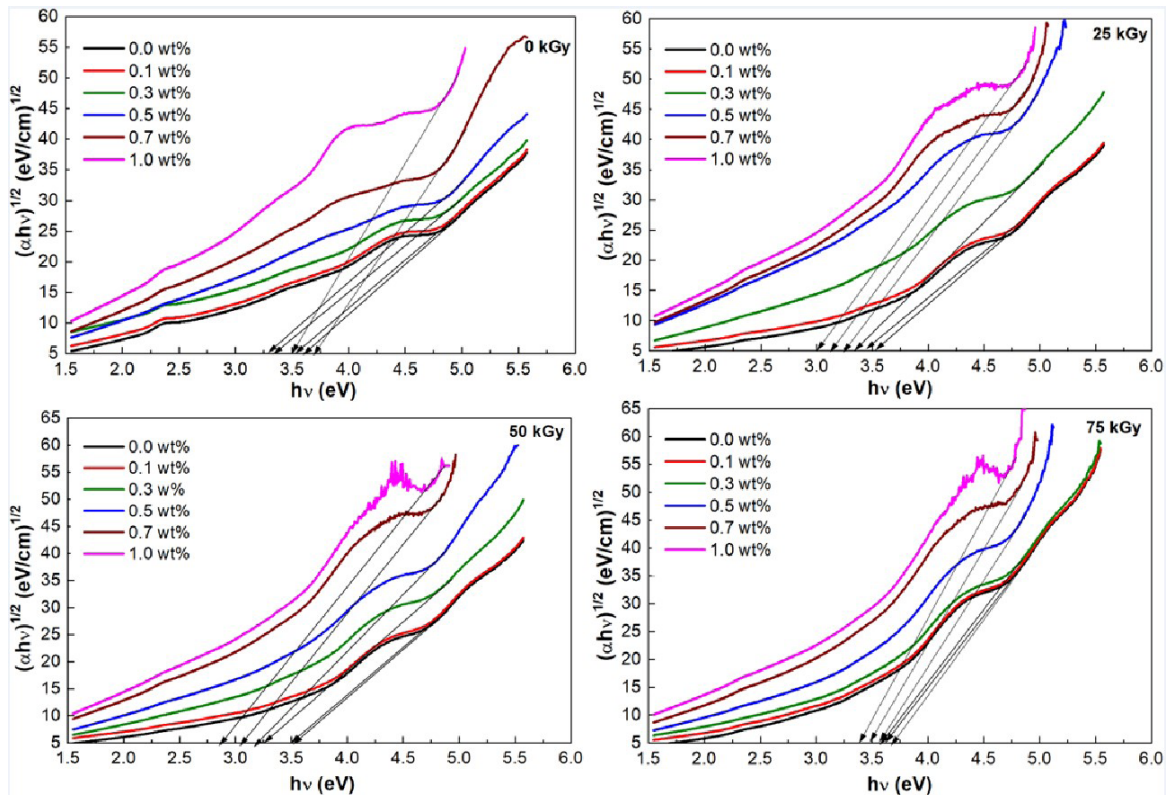
Figure 8. Plot of $(\alpha h\nu)^{1/2}$ versus $h\nu$ for irradiated and unirradiated PVC and PVC/ZnS films.

Table 3. Comparison of band gap values obtained from Tauc's method ($(\alpha h\nu)^2$ and $(\alpha h\nu)^{1/2}$) and from ε_i analysis.

ZnS (wt%)	E_g (eV)											
	0 kGy			25 kGy			50 kGy			75 kGy		
	2	1/2	εi	2	1/2	εi	2	1/2	εi	2	1/2	εi
0.0	4.67	3.62	4.22	4.63	3.51	4.20	4.65	3.53	4.12	4.79	3.70	4.08
0.1	4.59	3.56	4.17	4.55	3.44	4.13	4.62	3.52	4.01	4.72	3.65	4.04
0.3	4.51	3.37	4.05	4.49	3.31	3.92	4.43	3.29	3.93	4.68	3.61	3.97
0.5	4.46	3.27	4.03	4.48	3.29	3.81	4.42	3.19	3.82	4.62	3.57	3.79
0.7	4.62	3.72	4.05	4.42	3.14	3.61	4,38	3.06	3.72	4.46	3.45	3.52
1.0	4,51	3.53	4.04	4,41	2.99	3.57	4,31	2.88	3.57	4.42	3,42	3.31

The E_g= 4.67 eV (direct transition) and E_g=3.62 eV (indirect transition) were found for the unirradiated PVC films. These values decreased as increasing ZnS concentration function. The enhancement of carrier–carrier interaction due to the ZnS presence in valence and conduction bands leads to a reduction in the bandgap. Nonetheless, the lower E_g value was found for PVC/ZnS at 0.5 wt% (unirradiated samples). These results are attributed to the formation of localized states in the band gap by ZnS nanoparticles and are according to the electrical conductivity results shown in Table 1. Figure 9 represents the gap energies for direct and indirect transitions and the formation of the localized state due to ZnS incorporation at 0.5 wt% in an unirradiated

PVC matrix. Similar results were discussed for another PVC nanocomposite[26-30,41,47].

Furthermore, the radiation dose plays an important role in the E_g value for irradiated films. Figure 10 showed the behavior of E_g (direct and indirect transitions) in the ZnS concentration and irradiation dose function. Similar behavior was found for PVC and PVC/ZnS film, i. e., E_g value decreased as a function of dose increasing (until 50 kGy). Nevertheless, the E_g value is shifted to a higher value at 75 kGy. The radiolytic effects undergo formation defects in PVC molecules, resulting in different polymer chain lengths and consequently impacting optical band gap values[42,52]. The variation of the optical band gap infers
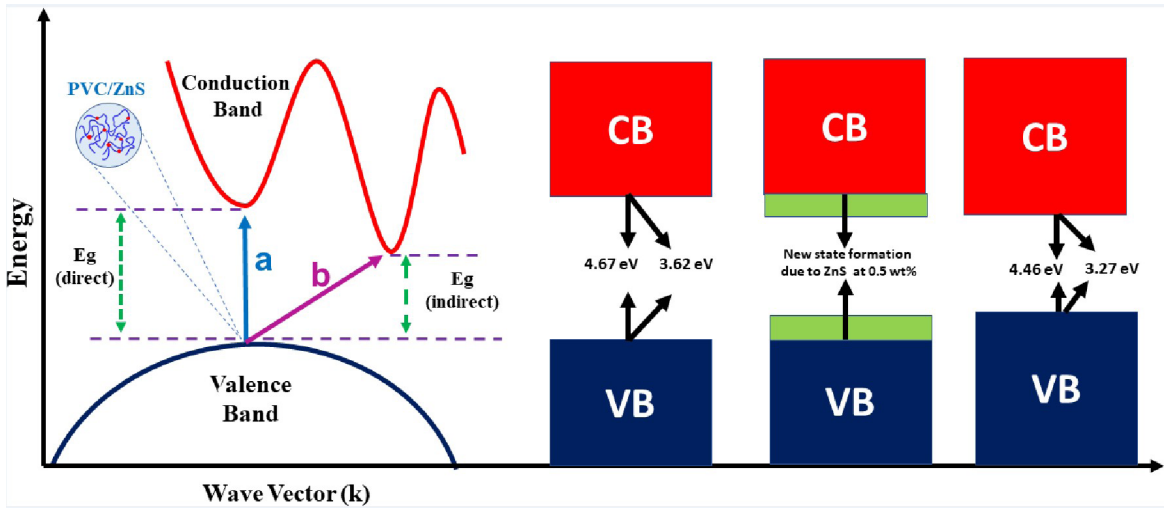
Figure 9. Representation of E_g for direct and indirect transitions and the formation of the localized state between the valence band (VB) and conduction band (CB).
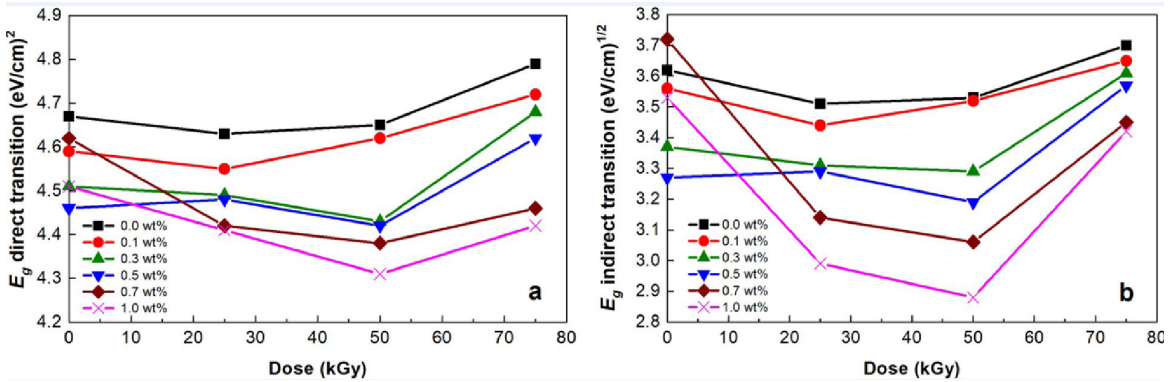
Figure 10. Influence of gamma irradiation on E_g value of PVC and PVC/ZnS films for a) direct allowed transition and b) indirect allowed transition.

that gamma irradiation modifies the electronic structure of nanocomposite samples by creating more free electrons in the conduction band.

On the other hand, E_U values (see Figure 11) for unirradiated PVC films were increased to increase the ZnS concentration. However, E_U values decreased at 0.1 and 0.3 wt% for all systems (irradiated and unirradiated). This effect was caused by a specific order of the nanoparticles, probably by the action of octadecylamine.

The effects of gamma radiation also cause an increase in the E_U value with the increase in irradiation dose. The increase in E_U values could be attributed to the rise in main chain structural disorder by ZnS and defects upon irradiation, leading to many possible band-to-tail and tail-to-tail transitions[63].

Furthermore, the decrease in E_g and the increase of the E_U in irradiated films reinforce the results obtained from electrical conductivity measurements. The decrease in Eg leads to an increase in the mobility of the ZnS, permitting it to hop from one site to another. It is attributed to the charge-transfer reaction in the interface of the film, which translates into an increase in film conductivity (see Table 1)[64,65].
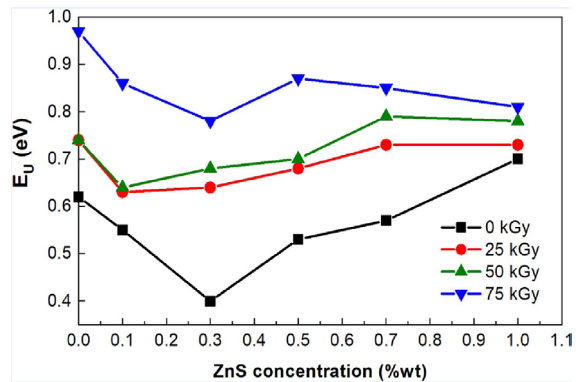
Figure 11. Influence of gamma radiation on E_U value of PVC and PVC/ZnS films.

The modifications in E_g and E_U also relate to forming a carbon cluster near the polymer surface. According to Figure 12, the number of carbon atoms per cluster in conjugate length (M) was changed as a function of ZnS concentration and radiation dose. For unirradiated samples, the increase
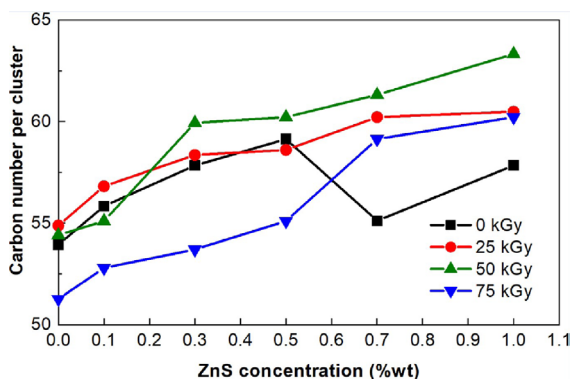
Figure 12. Effect of gamma radiation and ZnS concentration on the number of carbon atoms per conjugate length for band gap.

in M until 0.5 wt% concentration was found due to the modifications in the band gap by enriched domains created for the nanoparticles. Moreover, the M value was decreased at 0.7 and 1.0 wt%.

On the other hand, the M increased in films exposed to 25 and 50 kGy, then decreased to 75 kGy. The probable explanation is that the mechanism of scission (predominant at 25 and 50 kGy) and crosslinking (predominant at 75 kGy)[42] were responsible for different carbon domain formations. The increase of M at 25 and 50 kGy is attributed to cleavages of C–H and C-Cl bonds during the irradiation and, consequently, the formation of defects and new charge states[7]. The conjugated structures were formatted from the scission effect, while the crosslinking effect is responsible for the construction of chains longer and entanglement[52]. Thus, the PVC/ZnS films irradiated at 75 kGy showed minor carbon-enriched domains than those irradiated at lower doses. Consequently, this behavior may be responsible for the increase in the optical band gap (see Figure 10) with a consequent decrease in electrical conductivity of nanocomposites films irradiated at 75 kGy (Table 1).

4. Conclusion

Films of PVC/ZnS nanocomposites were prepared by solution casting technique. Using the octadecylamine surfactant enabled the film production to be more homogeneous and with better dispersion of ZnS. The effects of different amounts of ZnS and gamma radiation dose on the electrical and optical properties of the nanocomposite were studied. Our results showed that it is possible to make plastic-composite semiconductor material based on PVC only by adding ZnS nanoparticles at 0.5 wt%. Electrical conductivity increased in films irradiated at 25 kGy due scission effect, which contributed to the significant mobility of ZnS in the PVC matrix. The electrical conductivity measurement was reinforced by the different behavior of optical band gaps and Urbach's energy in the ZnS concentration and irradiation dose function.

The optical parameters also were influenced by ZnS content and gamma radiation dose. The optical conductivity, refraction index, and dielectric constant values increased in the ZnS concentration and irradiation dose function. These results indicate that the electrical and optical properties

of PVC/ZnS films can be easily modulated under gamma radiation. This way, PVC/ZnS nanocomposites with ZnS at lower concentrations and irradiated with gamma radiation at 25 kGy have potential use in optoelectronic devices. Thus, we obtained a nanocomposite material with a low concentration of nanoparticles, a semiconductor, which reduces costs and minimizes processing problems.

5. References

1. Petti L, Münzenrieder N, Vogt C, Faber H, Büthe L, Cantarella G et al. Metal oxide semiconductor thin-film transistors for flexible electronics. Appl Phys Rev. 2016;3:021303. http://dx.doi.org/10.1063/1.4953034.

2. Vikulov S, Stasio F, Ceseracciu L, Saldanha PL, Scarpellini A, Dang Z et al. Fully solution-processed conductive films based on colloidal copper selenide nanosheets for flexible electronics. Adv Funct Mater. 2016;26:3670-7. http://dx.doi.org/10.1002/adfm.201600124.

3. Gunda M, Kumar P, Katiyar M. Review of mechanical characterization techniques for thin films used in flexible electronics. Crit Rev Solid State Mater Sci. 2017;42:129-52. http://dx.doi.org/10.1080/10408436.2016.1186006.

4. Chen X, Han X, Shen QD. PVDF-based ferroelectric polymers in modern flexible electronics. Adv Electron Mater. 2017;3(5):1600460. http://dx.doi.org/10.1002/aelm.201600460.

5. Kleinschmidt AT, Lipomi DJ. Stretchable conjugated polymers: a case study in topic selection for new research groups. Acc Chem Res. 2018;51:3134-43. http://dx.doi.org/10.1021/acs.accounts.8b00459.

6. Zarek M, Layani M, Cooperstein I, Sachyani E, Cohn D, Magdassi S. 3D printing of shape memory polymers for flexible electronic devices. Adv Mater. 2016;28:4449-54. http://dx.doi.org/10.1002/adma.201503132.

7. Elamin AA, Elkanzi MHA, Hassan EA, Ahmed BE, Khareif ASM. Changes in electrical properties due to gamma irradiation of polyvinyl chloride (PVC). Am J Electromagn Appl. 2016;4:34-8. http://dx.doi.org/10.11648/j.ajea.20160402.14.

8. El-Shamy AG, Attia WM, Kader KMA. Enhancement of the conductivity and dielectric properties of PVA/Ag nanocomposite films using γ irradiation. Mater Chem Phys. 2017;191:225-9. http://dx.doi.org/10.1016/j.matchemphys.2017.01.026.

9. Puišo J, Adliene D, Guobiene A, Prosycevas I, Plaipaite-Nalivaiko R. Modification of Ag-PVP nanocomposites by gamma irradiation. Mater Sci Eng B. 2011;176:1562-7. http://dx.doi.org/10.1016/j.mseb.2011.05.003.

10. Sevil UA, Coşkun E, Güven O. Electrical conductivity and spectroscopic characterization of Blends of poly(2-chloroaniline)/polyaniline P(2ClANI)/PANI copolymer with PVC exposed to gamma-rays. Radiat Phys Chem. 2014;94:45-8. http://dx.doi.org/10.1016/j.radphyschem.2013.07.029.

11. Doyan AS. Effects of gamma radiation on electrical conductivity of PVA-CH composites. Mater Sci Forum. 2015;827:180-5. https://doi.org/10.4028/www.scientific.net/MSF.827.180.

12. Raghu S, Archana K, Sharanappa C, Ganesh S, Devendrappa H. Electron beam and gamma ray irradiated polymer electrolyte films: dielectric properties. J Radiat Res Appl Sci. 2016;9:117-24. http://dx.doi.org/10.1016/j.jrras.2015.10.007.

13. Freitas DMS, Araujo PLB, Araujo ES, Katia KA. Effect of copper sulfide nanoparticles in poly(vinyl chloride) exposed to gamma irradiation. J Inorg Organomet Polym Mater. 2017;27:1546-55. http://dx.doi.org/10.1007/s10904-017-0615-8.

14. Albuquerque MCC, Garcia OP, Aquino KAS, Araujo PLB, Araujo ES. Stibnite nanoparticles as a new stabilizer for poly (methyl methacrylate) exposed to gamma irradiation. Mater Res. 2015;18:978-83. http://dx.doi.org/10.1590/1516-1439.000814.

15. Bhavsar V, Tripathi D. Surface and dielectric studies of PVC-PVP blend films for green electronics. Indian J Pure Appl Phy. 2018;56:696-702.

16. Mohamed AT. Thermal experimental verification on effects of nanoparticles for enhancing electric and dielectric performance of polyvinyl chloride. Measurement. 2016;89:28-33. http://dx.doi.org/10.1016/j.measurement.2016.04.002.

17. Asha S, Sangappa Y, Ganesh S. Tuning the refractive index and optical band gap of silk fibroin films by electron irradiation. J Spectrosc. 2015;2015:879296. http://dx.doi.org/10.1155/2015/879296.

18. Lee EH, Rao GR, Mansur LK. LET effect on crosslinking and scission mechanisms of PMMA during irradiation. Radiat Phys Chem. 1999;55:293-305. http://dx.doi.org/10.1016/S0969-806X(99)00184-X.

19. Donahue EJ, Roxburgh A, Yurchenko M. Sol-gel preparation of zinc sulfide using organic dithiols. Mater Res Bull. 1998;33:323-9. http://dx.doi.org/10.1016/S0025-5408(97)00232-8.

20. Fang X, Zhai T, Gautam UK, Li L, Wu L, Bando Y et al. ZnS nanostructures: from synthesis to applications. Prog Mater Sci. 2011;56:175-287. http://dx.doi.org/10.1016/j.pmatsci.2010.10.001.

21. Silva RC, Silva LA, Araújo PLB, Araújo ES, Santos RFS, Aquino KAS. ZnS nanocrystals as an additive for gamma-irradiated poly (vinyl chloride). Mater Res. 2017;20:851-7. http://dx.doi.org/10.1590/1980-5373-mr-2016-0983.

22. Von Blythe AR. Electrical properties of polymers. 2nd ed. Cambrige: Cambrige University Press; 2005.

23. SEMI. SEMI MF43-0705: test method for resistivity of semiconductor materials. Milpitas: SEMI; 2005.

24. Stevens MP. Polymer chemistry: an introduction. 3rd ed. Oxford: Oxford University Press; 1999.

25. Tauc J. Amorphous and liquid semiconductor. Boston: Springer; 1974.

26. Mahmoud WE. Morphology and physical properties of poly(ethylene oxide) loaded graphene nanocomposites prepared by two different techniques. Eur Polym J. 2011;47:1534-40. http://dx.doi.org/10.1016/j.eurpolymj.2011.05.011.

27. Davis EA, Mott NF. Conduction in non-crystalline systems V. Conductivity, optical absorption and photoconductivity in amorphous semiconductors. Philos Mag. 1970;22(179):0903-0922. https://doi.org/10.1080/14786437008221061.

28. El-Deen LMS, Salhi MSA, Elkholy MM. IR and UV spectral studies for rare earths-doped tellurite glasses. J Alloys Compd. 2008;465:333-9. http://dx.doi.org/10.1016/j.jallcom.2007.10.104.

29. Reddeppa N, Sharma AK, Rao VVRN, Chen W. Preparation and characterization of pure and KBr doped polymer blend (PVC/PEO) electrolyte thin films. Microelectron Eng. 2013;112:57-62. http://dx.doi.org/10.1016/j.mee.2013.05.015.

30. Wen R, Wang L, Wang X, Yue GH, Chen Y, Peng DL. Influence of substrate temperature on mechanical, optical and electrical properties of ZnO:Al films. J Alloys Compd. 2010;508:370-4. http://dx.doi.org/10.1016/j.jallcom.2010.08.034.

31. Hussein AM, Dannoun EMA, Aziz SB, Brza MA, Abdulwahid RT, Hussen SA et al. Steps toward the band gap identification in polystyrene based solid polymer nanocomposites integrated with tin titanate nanoparticles. Polymers. 2020;12:1-21. http://dx.doi.org/10.3390/polym12102320.

32. Hashim A, Hadi Q. Synthesis of novel (polymer blend-ceramics) nanocomposites: structural, optical and electrical properties for humidity sensors. J Inorg Organomet Polym Mater. 2018;28:1394-401. http://dx.doi.org/10.1007/s10904-018-0837-4.

33. Yousif E, Abdallh M, Hashim H, Salih N, Salimon J, Abdullah BM et al. Optical properties of pure and modified poly(vinyl chloride). Int J Ind Chem. 2013;4:1-8. http://dx.doi.org/10.1186/2228-5547-4-4.

34. Fink D. Angle X-ray scattering and ESR. Nucl Instrum Methods Phys Res. 1996;111:303-14.

35. Urbach F. The long-wavelength edge of photographic sensitivity and of the electronic Absorption of Solids. Phys Rev J Arch. 1953;92:1324. http://dx.doi.org/10.1103/PhysRev.92.1324.

36. Migahed MD, Zidan HM. Influence of UV-irradiation on the structure and optical properties of polycarbonate films. Curr Appl Phys. 2006;6:91-6. http://dx.doi.org/10.1016/j.cap.2004.12.009.

37. Yahia IS, Farag AAM, Cavas M, Yakuphanoglu F. Effects of stabilizer ratio on the optical constants and optical dispersion parameters of ZnO nano-fiber thin films. Superlattices Microstruct. 2013;53:63-75. http://dx.doi.org/10.1016/j.spmi.2012.09.008.

38. Ubale AU, Sangawar VS, Kulkarni DK. Size dependent optical characteristics of chemically deposited nanostructured ZnS thin films. Bull Mater Sci. 2007;30:147-51. http://dx.doi.org/10.1007/s12034-007-0026-5.

39. Omar MA. Elementary solid state physics. Boston: Addison-Wesley Publishing Company; 1987.

40. Pankove JI. Optical processes in semiconductors. 2nd ed. New York: Dover Publications Inc; 2010.

41. Seanor DA. Electrical properties of polymers. New York: Elsevier; 1982. Electrical conduction in polymers; pp. 1-58.

42. Silva FF, Aquino KA, Araújo ES. Effects of gamma irradiation on poly(vinyl chloride)/polystyrene blends: investigation of radiolytic stabilization and miscibility of the mixture. Polym Degrad Stabil. 2008;93:2199-203. http://dx.doi.org/10.1016/j.polymdegradstab.2008.07.024.

43. Zaki MF. Gamma-induced modification on optical band gap of CR-39 SSNTD. Braz J Phys. 2008;38:558-62. http://dx.doi.org/10.1590/S0103-97332008000500005.

44. Al-Taa'y WA, Abdulnabi MT, Al-Rawi TK. The MR affect on optical properties for poly (Vinyl alcohol) films. Baghdad Sci J. 2011;8:543-50. http://dx.doi.org/10.21123/bsj.8.2.543-550.

45. Sangappa, Asha S, Demappa T, Sanjeev G, Parameswara P, Somashekar R. Spectroscopic and thermal studies of 8 MeV electron beam irradiated HPMC films. Nucl Instrum Methods Phys Res B. 2009;267:2385-9. http://dx.doi.org/10.1016/j.nimb.2009.04.007.

46. Baltova S, Vassileva V, Valtcheva E. Photochemical behaviour of natural silk - I. Kinetic investigation of photoyellowing. Polym Degrad Stabil. 1998;60:53-60. http://dx.doi.org/10.1016/S0141-3910(97)00016-5.

47. Mohamod KG. Council for innovative research. J Adv Chem. 2014;10:2146-61.

48. Rajulu AV, Reddy RL, Raghavendra SM, Ahmed SA. Miscibility of PVC/PMMA blend by the ultrasonic and refractive index method. Eur Polym J. 1999;35:1183-6. http://dx.doi.org/10.1016/s0014-3057(98)00078-0.

49. Nouh SA, Abdel-Salam MH, Morsy AA. Electrical, optical and structural behaviour of fast neutron-irradiation-induced CR-39 SSNTD. Radiat Meas. 2003;37:25-9. http://dx.doi.org/10.1016/S1350-4487(02)00122-1.

50. Kim DH, Viventi J, Amsden JJ, Xiao J, Vigeland L, Kim YS et al. Dissolvable films of silk fibroin for ultrathin conformal bio-integrated electronics. Nat Mater. 2010;9:1-7. http://dx.doi.org/10.1038/nmat2745.

51. Tao H, Brenckle MA, Yang M, Zhang J, Liu M, Siebert SM et al. Silk-based conformal, adhesive, edible food sensors. Adv Mater. 2012;24:1067-72. http://dx.doi.org/10.1002/adma.201103814.

52. Eid S, Ebraheem S, Abdel-Kader NM. Study the effect of gamma radiation on the optical energy gap of poly(vinyl alcohol) based ferrotitanium alloy film: its possible use in radiation dosimetry. Open J Polym Chem. 2014;4:21-30. http://dx.doi.org/10.4236/ojpchem.2014.42003.

53. Tahir KJ. Effect of gamma irradiation on optical properties of CdS thin films. J Univ Kerbala. 2017;15(1):49-55.

54. Mansour AF, Mansour SF, Abdo MA. Improvement structural and optical properties of ZnO/ PVA nanocomposites. IOSR J Appl Phys. 2015;7:60-9. http://dx.doi.org/10.9790/4861-07226069.

55. Aziz SB, Marif RB, Brza MA, Hassan AN, Ahmad HA, Faidhalla YA et al. Structural, thermal, morphological and optical properties of PEO filled with biosynthesized Ag nanoparticles: new insights to band gap study. Results Phys. 2019;13:102220. http://dx.doi.org/10.1016/j.rinp.2019.102220.

56. Abdullah RM, Aziz SB, Mamand SM, Hassan AQ, Hussein SA, Kadir MFZ. Reducing the crystallite size of spherulites in PEO-based polymer nanocomposites mediated by carbon nanodots and Ag nanoparticles. Nanomaterials. 2019;9(6):874. http://dx.doi.org/10.3390/nano9060874.

57. Aziz SB. Morphological and optical characteristics of chitosan(1−x):Cuox (4 ≤ x ≤ 12) based polymer nano-composites: optical dielectric loss as an alternative method for tauc's model. Nanomaterials. 2017;7(12):444. http://dx.doi.org/10.3390/nano7120444.

58. Aziz SB, Rasheed MA, Ahmed HM. Synthesis of polymer nanocomposites based on [methyl cellulose](1-x):(CuS)x (0.02M ≤ x ≤ 0.08 M) with desired optical band gaps. Polymers. 2017;9(6):194. http://dx.doi.org/10.3390/polym9060194.

59. Hu CE, Zeng ZY, Cheng Y, Chen XR, Cai LC. First-principles calculations for electronic, optical and thermodynamic properties of ZnS. Chin Phys B. 2008;17:3867-74. http://dx.doi.org/10.1088/1674-1056/17/10/053.

60. Rahman MA, Rahman MA, Chowdhury UK, Bhuiyan MTH, Ali ML, Sarker MAR. First principles investigation of structural, elastic, electronic and optical properties of ABi2O6 (A=Mg, Zn) with trirutile-type structure. Cogent Phys. 2016;3(1):1257414 http://dx.doi.org/10.1080/23311940.2016.1257414.

61. Nasr TB, Maghraoui-Meherzi H, Abdallah HB, Bennaceur R. First principles calculations of electronic and optical properties of Ag2S. Solid State Sci. 2013;26:65-71. http://dx.doi.org/10.1016/j.solidstatesciences.2013.09.017.

62. Zhao XY, Wang YH, Zhang M, Zhao N, Gong S, Chen Q. First-principles calculations of the structural, electronic and optical properties of BaZrxTi1-xO3 (x = 0, 0.25, 0.5, 0.75). Chin Phys Lett. 2011;28:1-5. http://dx.doi.org/10.1088/0256-307X/28/6/067101.

63. O'Leary SK, Zukotynski S, Perz JM. Disorder and optical absorption in amorphous silicon and amorphous germanium. J Non-Cryst Solids. 1997;210:249-53. http://dx.doi.org/10.1016/S0022-3093(96)00612-6.

64. Singh VP, Ramani R, Pal V, Prakash A, Alam S. Microstructure and properties of novel fluorescent pyrene functionalized PANI/P(VDF-HFP) blend. J Appl Polym Sci. 2014;131:1-11. http://dx.doi.org/10.1002/app.40163.

65. Ghamsari MS, Bidzard AM, Han W, Park H-H. Wavelength-tunable visible to near-infrared photoluminescence of carbon dots: the role of quantum confinement and surface states. J Nanophotonics. 2016;10:026028. http://dx.doi.org/10.1117/1.jnp.10.026028.